symmetry

MDPI

Article

Heat Transfer Characteristics of an Electric Motor with Oil-Dripping Cooling under Overload Conditions

Eun-Hyeok Kang, Kunal Sandip Garud, Su Cheong Park and Moo-Yeon Lee *

Department of Mechanical Engineering, Dong-A University, 37 Nakdong-Daero 550, Saha-gu, Busan 49315, Republic of Korea; 2270089@donga.ac.kr (E.-H.K.); 1876936@donga.ac.kr (K.S.G.); park@dau.ac.kr (S.C.P.)
* Correspondence: mylee@dau.ac.kr; Tel.: +82-51-200-7642

Abstract: The continuously increasing energy density of electric motors to match the performance of electric vehicles with internal-combustion-engine vehicles demands an advanced cooling strategy. Direct dripping/spray cooling is one of such potential cooling strategies to replace the conventional cooling method for achieving the desired thermal management of next-generation electric motors. In the present work, the heat transfer characteristics of an electric motor with oil-dripping cooling were experimentally investigated considering overload operating conditions. An experimental set-up comprising a 15 kW electric motor and an oil-dripping cooling system was developed. The experimental data were used to evaluate the maximum temperature, heat transfer coefficient and power consumption under the influence of a dripping hole diameter (2 mm, 3 mm, 4 mm), oil flow rate (8 LPM, 12 LPM, 16 LPM) and overload operating power (8.28 kW, 12.05 kW, 14.21 kW). The symmetrical oil distribution over the electric motor and the superior heat transfer from the electric motor to the oil was achieved when the oil-dripping cooling system was designed with the combination of a 4 mm dripping hole diameter and a 12 LPM oil flow rate. The combination of the 4 mm dripping hole diameter and 12 LPM oil flow rate showed the lowest maximum temperatures of 31.9 °C and 46.3 °C for electric motor under overload operating powers of 8.28 kW and 14.21 kW, respectively. In addition, the highest heat transfer coefficient of 7528.61 W/m^2-K and lowest power consumption of 18.07 W were achieved for the oil-dripping cooling system with the combination of a 4 mm dripping hole diameter and 12 LPM oil flow rate. The best combination of the operating parameters is proposed for developing the oil-dripping cooling system that enables superior heat transfer characteristics and, thus, an enhanced thermal management of electric motors under overload conditions.

Keywords: dripping hole diameter; electric motor; heat transfer characteristics; oil-dripping cooling; overload operating power

Citation: Kang, E.-H.; Garud, K.S.; Park, S.C.; Lee, M.-Y. Heat Transfer Characteristics of an Electric Motor with Oil-Dripping Cooling under Overload Conditions. *Symmetry* **2024**, *16*, 289. https://doi.org/10.3390/sym16030289

Academic Editor: Chong Wang

Received: 13 February 2024
Revised: 26 February 2024
Accepted: 28 February 2024
Published: 1 March 2024

1. Introduction

The global greenhouse gas emissions including carbon dioxide (CO_2), sulfur dioxide (SO_2), nitrogen oxides (NO_x), carbon monoxide (CO) and particulate matter (PM) are increasing owing to the excessive consumption of fossil fuel-based energy sources [1]. The transportation sector has the second-largest greenhouse gas emissions which has led to the imposing of several regulations by various governments to ensure a carbon-free future [2]. Therefore, the current transportation sector is facing the rapid transition to electric mobility as a sustainable future for replacing the fossil fuel-based vehicles [3,4].

An electric motor is the key integral driving component that assures the traction of electric vehicles. The performance and reliability of electric vehicles could be improved by enhancing the torque and efficiency of electric motors [5]. To ensure a miniaturized electric vehicle driving system, the size of electric motors has become compact, which has resulted in increased energy density. A significant portion of the energy is dissipated in the form of heat owing to various losses in such high-power density electric motors [6]. The high

heat generation could cause the demagnetization of magnets and insulation aging and, thus, the reduced torque rating and efficiency of electric motors. Furthermore, excessive heat generation could reduce the life span of electric motors, and in several cases, it could result in permanent damage with burnout [7]. Therefore, cooling strategies are applied to electric motors to dissipate the heat generation and maintain the optimum performance of the electric motor [8,9]. The conventionally used water jacket cooling fails to maintain the desired thermal management, as the power density of electric motors is increasing because of increased thermal resistance owing to the presence of indirect cooling channels [10,11]. An advanced thermal management technology should be developed with the benefits of minimal thermal resistance and enhanced cooling for next-generation electric motors. In the search for advanced cooling strategies, direct liquid cooling in forms of direct cooling channels and direct dripping/spray cooling is gaining popularity.

Acquaviva et al. [12] (2020) proposed in-stator and in-slot direct oil cooling for the thermal management of electric motors with a tooth coil winding. Maximum winding temperatures of 170 °C and 200 °C were reported for the continuous and peak operations, respectively, for the proposed cooling. Lindh et al. [13] (2017) reported temperature rises of 110 °C, 60 °C and 31 °C for windings in the case of indirect water, direct oil and direct water cooling, respectively. The efficiency of the motor was evaluated as 95% for direct water cooling and just above 94% for indirect water cooling. Venturini et al. [14,15] (2020 & 2021) compared the performance of electric motor in different configurations of in-slot water cooling channels. One of the configurations showed the lowest magnetic and winding temperatures of 108 °C and 106 °C with an efficiency of 93.72%. Park et al. [16] (2022) demonstrated the superiority of direct slot cooling with a 66%, 94% and 35% higher current density compared to water jacket cooling, end-tip cooling and channel cooling, respectively. Huang et al. [17] (2012) reduced the average temperature of a stator by a factor of two for direct cooling with grooves between stator and housing compared to indirect water jacket cooling. The manufacturing of direct cooling channels within electric motors involves complexity in terms of structural alterations; hence, researchers are also exploring the feasibility and practical reliability of direct spray/dripping cooling for electric motors [18,19].

Davin et al. [20] (2015) observed that the dripping injection affects the global cooling performance, whereas the jet injection is restricted to the local cooling performance for a motor's end windings. The dripping injection reduces the average temperature of end windings up to 109 °C. The global heat transfer efficiency of motor cooling is significantly affected by flow rate compared to rotational speed. Ponomarev et al. [21] (2012) immersed the motor in oil, which reduces the maximum temperature to 124 °C due to an enhanced heat transfer rate from the motor to the oil. Rocca et al. [22] (2021) proposed a combined water jacket with spray cooling and noted that the number of nozzles, nozzle location and spray angle affect the spray-cooling performance of electric motors. Guechi et al. [23] (2013) observed that the heat dissipation performance of spray cooling using water is superior for stator winding surrounded with air compared to that with a higher-thermal-conductivity resin. The influence of water inlet temperature and flow rate on the spray cooling performance was evaluated. Wang et al. [24] (2018) studied the heat transfer characteristics of the spray cooling system, considering heat source equivalent to four electric motors under the influence of inlet temperature, flow rate and heat generation.

The reviewed literature shows that numerous research works have been onducted to study the thermal performances of electric motors with direct spray/dripping cooling considering various operating conditions. However, to ensure the commercial sustainability of direct spray/dripping cooling for electric motors, their performance should be evaluated under harsh operating conditions, which has not been explored till date. Therefore, the present study investigated the heat transfer characteristics of an electric motor with an oil-dripping cooling system under overload operating powers. Furthermore, the innovation of this work involves an experimental study to analyze the effect of dripping hole diameter and oil flow rate on heat transfer characteristics. In addition, the maximum temperature,

heat transfer coefficient, and power consumption were analyzed considering dripping hole diameters of 2 mm, 3 mm and 4 mm; oil flow rates of 8 LPM, 12 LPM and 16 LPM, and overload operating powers of 8.28 kW, 12.05 kW and 14.21 kW. As a result, the best combination of dripping hole diameter and oil flow rate is proposed to develop the oil-dripping cooling system with the aim of achieving a symmetrical oil distribution and improved heat transfer characteristics for electric motors.

2. Experimental Methodology

2.1. Description of Experimental Set-Up

A schematic diagram of the experimental set-up for an electric motor with oil-dripping cooling system is depicted in Figure 1. A 15 kW three-phase electric motor is considered as the target motor in the present experimental work. The configuration of the electric motor comprises stranded windings in stator, four poles and a squirrel cage-type rotor. In the proposed oil-dripping cooling system, the oil is sprayed on the electric motor through the holes in the cooling tube. The cooling tubes for dripping were manufactured with hole diameters of 2 mm, 3 mm and 4 mm, respectively. Two cooling tubes with the same length as that of the electric motor are created with these holes, such that the oil is sprayed uniformly over the electric motor. These two main cooling tubes are connected through smaller tubes with a common inlet and outlet. The commonly used transmission oil in automobiles of type ATF-SP4M1 was selected as a coolant for oil the dripping cooling system. The properties of the ATF oil are presented in Table 1 [25]. The windings enable the largest heat generation in an electric motor; hence, each main cooling tube is designed with two dripping holes on each side of the end windings and two center holes equally spaced over the stator. Thus, both main cooling tubes are arranged symmetrically to enable the uniform distribution of oil over the electric motor targeting a maximum portion of the windings followed by other components of the electric motor. The electric motor with an oil-dripping cooling system is housed within a chamber made of steel. Four steel plates of 600 mm $\times$ 600 mm $\times$ 600 mm are welded together to form this chamber. The electric motor is attached with T-type thermocouples enabling a temperature range of 0–400 °C. The pump with a 400 W capacity and maximum flow rate of 21.6 LPM is used to circulate the ATF oil in the cooling system. The flow rate of the circulating oil can be controlled using the regulator (inverter) connected with the pump. The regulator (inverter) controls the motor rpm of the pump, which helps to adjust the flow rate of the circulating oil based on the requirements of the oil-dripping cooling system. The oil enters into the common inlet of the oil-dripping tubes and, then, is distributed to each hole through the cooling tube. The pumped oil from the holes of the cooling tubes is sprayed on the electric motor. The oil is collected in the reservoir through the outlet of the base plate and recirculated after passing through a chiller with -25 °C to 80 °C temperature range. The 20 kW/hr heat exchanger is used to circulate the hot oil from the oil-dripping cooling system and cold water from the chiller. The flow circuit for oil circulation is made of rubber tube to withstand the high-pressure and -temperature requirements. The temperature and pressure of oil circulating through the chamber and chiller/heat exchanger are monitored using Pt-100 temperature sensors with a 0–850 °C temperature range and EDS.305 pressure sensors with a pressure range of -1 to 50 bar. The variable frequency inverter with a capacity of 15 kW and 380 V is used to control the power input to the electric motor. The speed of the rotating shaft of the electric motor is monitored through the inverter controller. The GL820 data logger with a temperature range of -200 to 850 °C and voltage range of 0 to 20 V is used to monitor and record the experimental data.

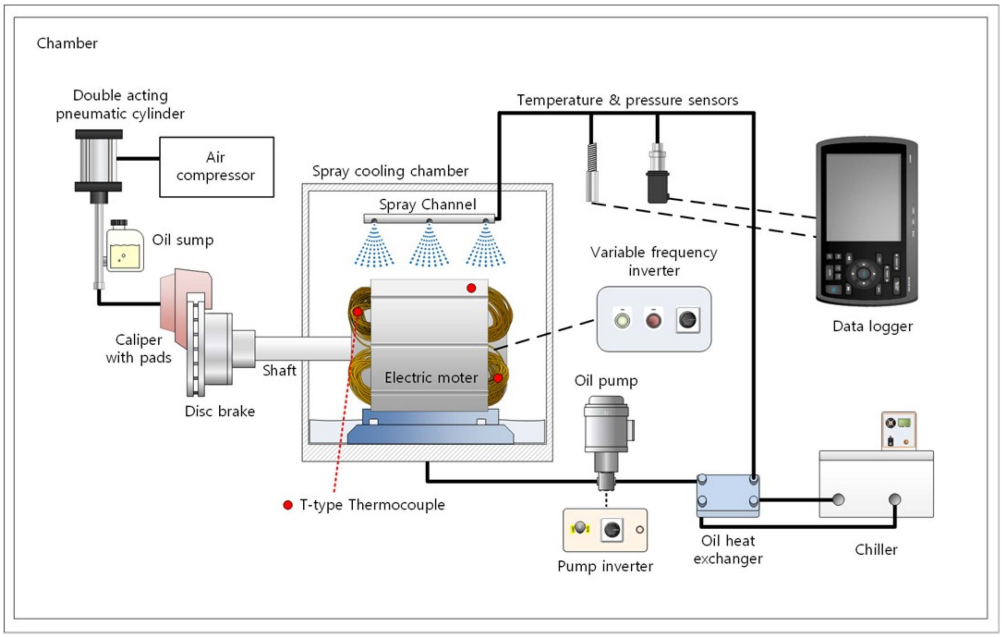

Figure 1. Schematic diagram of experimental set-up for electric motor with oil-dripping cooling system.

Table 1. Properties of ATF oil.

Property	Value
Density (kg/m^3)	829.5
Specific heat (J/kg-K)	1978.7
Viscosity (m^2/s)	2.21×10^{-5}
Thermal conductivity (W/m-K)	0.136

The brake dynamometer comprising disc brake and pads, piston caliper with oil tube and oil sump, pneumatic cylinder and air compressor is intended to enable the load on the electric motor. The air compressor with a capacity of 2.5 kW and maximum operating pressure of 8 bar is used to supply the air with pressure. The air supply from the compressor could be controlled using the regulator; thus, the air pressure at the outlet could be adjusted based on required conditions. An 80 mm pneumatic cylinder is provided with two control valves at the inlet and outlet, which are connected to the control switch through polyethylene air lines. The other end of the control switch is connected to the outlet of the air compressor using polyethylene air lines. Using the control valves and control switch, the push rod within the pneumatic cylinder could be moved in and out with generated air pressure from air compressor in both directions. The push rod of the pneumatic cylinder is connected to a brake lever with a brake oil sump. The in and out motions of the push rod generate the pressure on brake lever, which forces the oil from the oil sump against the piston through the oil tube. This piston within the brake caliper pushes the brake pad against the disc using the generated oil pressure and, thus, friction is generated across the disc, which reduces the speed of the electric motor. The friction on the brake side generates the heat, which must be dissipated for the continuous operation of the brake dynamometer. Therefore, forced air cooling is provided to maintain the temperature of the disc brake within a safe operating temperature range. The experimental set-up of the electric motor with an oil-dripping cooling system is housed within a constant-temperature chamber which, maintains the atmosphere's temperature in the range of 25 °C ± 0.5 °C.

2.2. Experimental Parameters and Uncertainty Analysis

The maximum temperature, heat transfer coefficient and power consumption were evaluated as heat transfer characteristics of the electric motor with an oil-dripping cooling

system. Liu et al. and Chong et al. suggested that the cooling performance for dripping/spray cooling is affected by coolant flow rate and coolant flow distribution [26,27]. Therefore, the heat transfer characteristics were analyzed considering a variation in the dripping hole diameter and oil flow rate under the influence of different overload operating powers.

The overload operating power (P_i) of an electric motor can be calculated as [28]

$$P_i = \frac{\sqrt{3} \cdot V \cdot I}{1000} \tag{1}$$

Here, V is the RMS voltage (input mean line to line voltage of three phases), and I is the RMS current (input mean current of three phases) supplied to the electric motor.

It should be noted that the brake load applied to the electric motor is adjusted to maximum, ensuring that there is no rotation of the electric motor shaft. Hence, it is considered that the amount of input power supplied is converted to the heat generation of the electric motor. However, there is minimal heat generation on the brake side, which is dissipated using fan cooling and is not considered in the electric motor's heat generation.

The heat transfer coefficient (h) is evaluated as [29]

$$P_i = h \cdot A \cdot \left(T_{motor,avg} - T_{oil,in}\right) \tag{2}$$

$$h = \frac{P_i}{2 \cdot \prod \cdot r_{motor,o} \cdot L \cdot \left(T_{motor,avg} - T_{oil,in}\right)} \tag{3}$$

Here, $r_{motor,o}$ is the outer radius of the electric motor, L is length of the motor, $T_{motor,avg}$ is the average temperature of the electric motor and $T_{oil,in}$ is the inlet temperature of the oil. The electric motor's average temperature can be calculated as an average of the components' temperatures including stator and windings.

The pumping power is obtained as [30]

$$P_{pumping} = p_{spray} \cdot \dot{V} \tag{4}$$

Here, p_{spray} is spray pressure, and $\dot{V}$ is volume flow rate of oil.

During the experimentation, obtained results deviate from the actual results owing to the errors in the prob position and calibration, measurement errors, accuracy of measuring devices and errors associated with ambient conditions [31]. The deviation between actual and obtained results is termed uncertainty in experimental parameters. Therefore, uncertainty analysis is conducted to ensure the reliability of the experimental results. In the present study, the linearized fraction approximation concept is used to determine the uncertainties in the extracted experimental data of the electric motor with an oil-dripping cooling system [32]. The thermocouples, data logger, pressure sensor and current meter offer accuracies of ±0.5%, ±0.1%, ±0.25% and ±0.2%, respectively. Equation (5) is used to evaluate the uncertainty in the dependent parameters by reflecting the uncertainties in various independent parameters in a combined way [33]. The uncertainties in temperature, heat transfer coefficient and power consumption are evaluated as ±1.76%, ±3.81% and ±3.26%, respectively.

$$U_Y = \sqrt{\left(\frac{\partial Y}{\partial X_1} \cdot U_{X1}\right)^2 + \left(\frac{\partial Y}{\partial X_2} \cdot U_{X2}\right)^2 + \left(\frac{\partial Y}{\partial X_3} \cdot U_{X3}\right)^2 + \ldots + \left(\frac{\partial Y}{\partial X_n} \cdot U_{Xn}\right)^2} \tag{5}$$

The uncertainty in the dependent parameter is presented as U_Y, and uncertainties in various independent parameters are reflected as U_{X1}, U_{X2}, U_{X3},..., U_{Xn}. The dependent parameter is presented as Y, and the independent parameters are termed as X_1, X_2, X_3...,X_n.

3. Results and Discussion

The heat transfer characteristics of the electric motor with an oil-dripping cooling system, in terms of maximum temperature, heat transfer coefficient and power consumption, are discussed under the effect of the dripping hole diameter at various overload operating powers in Section 3.1, and those under the effect of the oil flow rate at various overload operating powers are discussed in Section 3.2.

3.1. Effect of Dripping Hole Diameter at Various Overload Operating Powers

The dripping hole diameters were varied as 2 mm, 3 mm and 4 mm to investigate various heat transfer characteristics considering three overload operating powers of 8.28 kW, 12.05 kW and 14.21 kW, respectively.

3.1.1. Maximum Temperature

The variation in the maximum temperature for various dripping hole diameters and overload operating powers is shown in Figure 2. The maximum temperature of the electric motor is maintained within the permissible operating limit considering the F-class insulation for each dripping hole diameter under various overload operating powers. With an increase in the overload operating power, the heat generation loss increases, which results in the increase in the maximum temperature in for each dripping hole diameter. The flow distribution of oil on the electric motor is affected by change in dripping hole diameter, which indicates that a symmetrical oil flow distribution could reduce the maximum temperature of the electric motor. The dripping hole diameter of 4 mm depicts the lowest maximum temperature compared to other dripping hole diameters for all overload operating powers. It should be noted that in the case of higher overload operating powers of 12.05 kW and 14.21 kW, the dripping hole diameters of 3 mm and 4 mm show the maximum temperature almost in the same range; however, considering all overload operating powers, the dripping hole diameter of 4 mm is suggested to achieve the uniform oil flow distribution and lower maximum temperature of the electric motor. Considering the failure of the electric motor under various overload operating powers, the experiments were conducted for a duration of 10 min. The maximum temperatures of 36.2 °C, 39 °C and 31.9 °C in the case of 8.28 kW; 47.5 °C, 40.3 °C and 40.2 °C in the case of 12.05 kW; and 57.7 °C, 48.3 °C and 46.3 °C in case of 14.21 kW are observed for the dripping hole diameters of 2 mm, 3 mm and 4 mm, respectively.

3.1.2. Heat Transfer Coefficient

The heat transfer coefficient variation with the change in dripping hole diameter under various overload operating powers is presented in Figure 3. The heat transfer coefficient is evaluated considering the overall temperature of the electric motor. As the dripping hole diameter increases, it enlarges the oil distribution coverage area over the electric motor. Hence, the overall temperature of the electric motor reduces when the dripping hole diameter increases. The lower temperature of the electric motor indicates that a higher amount of heat is being transferred to the oil that is dripping through cooling tubes. The dripping hole diameter of 4 mm depicts a lower temperature of electric motor, which results in a higher heat transfer coefficient compared to other dripping hole diameters under each overload operating power. However, it should also be noticed that the heat transfer coefficients for dripping hole diameters of 3 mm and 4 mm are in the same range in the case of higher overload operating powers. The heat generation increases with the increase in the overload operating power; thus, the temperature of the electric motor is high at the higher overload operating power as reflected in terms of maximum temperature in the previous section. It is noticed that the oil is not able to absorb a significant portion of heat from the available quantity of heat generation as its amount increases. This means that the heat absorbed by the oil from the available heat generation at the overload operating powers of 12.05 kW and 14.21 kW is lower than that absorbed by the oil from the available heat generation at overload operating power of 8.28 kW. Hence, a larger amount of heat remains unabsorbed

at higher overload operating power, and, thus, the heat transfer coefficient decreases as the overload operating power increases in the case of each dripping hole diameter. The heat transfer coefficients of 4595.39 W/m^2-K, 5457.76 W/m^2 -K and 7528.61 W/m^2-K in the case of 8.28 kW; 3548.52 W/m^2-K, 4908.13 W/m^2-K and 4684.69 W/m^2-K in the case of 12.05 kW; and 3197.83 W/m^2-K, 3178.29 W/m^2-K and 3866.59 W/m^2-K in the case of 14.21 kW are evaluated for dripping hole diameters of 2 mm, 3 mm and 4 mm, respectively.

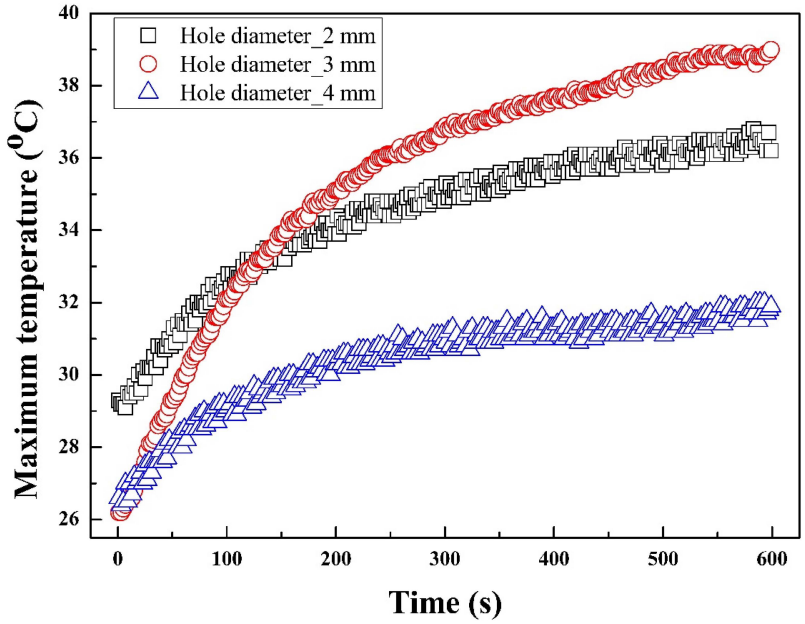

(**a**) Overload operating power of 8.28 kW

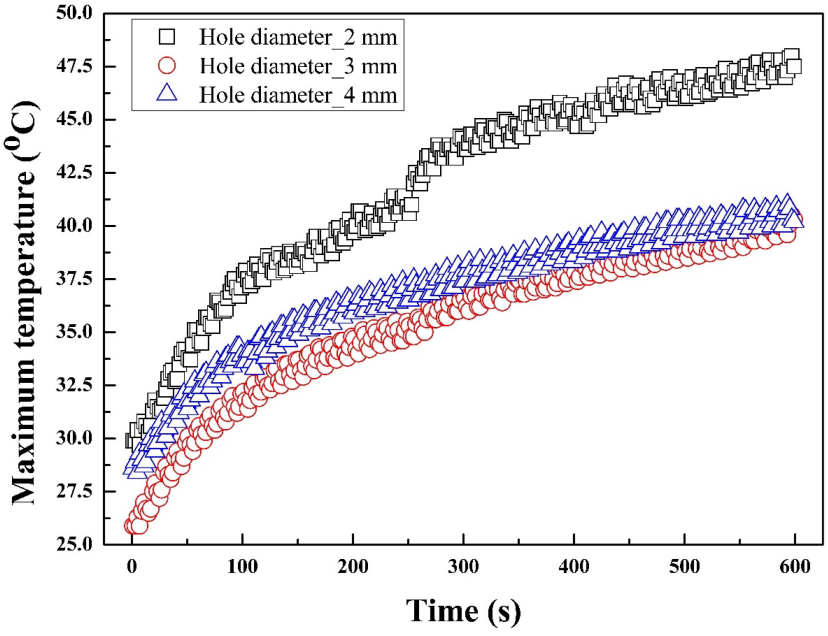

(**b**) Overload operating power of 12.05 kW

Figure 2. *Cont.*

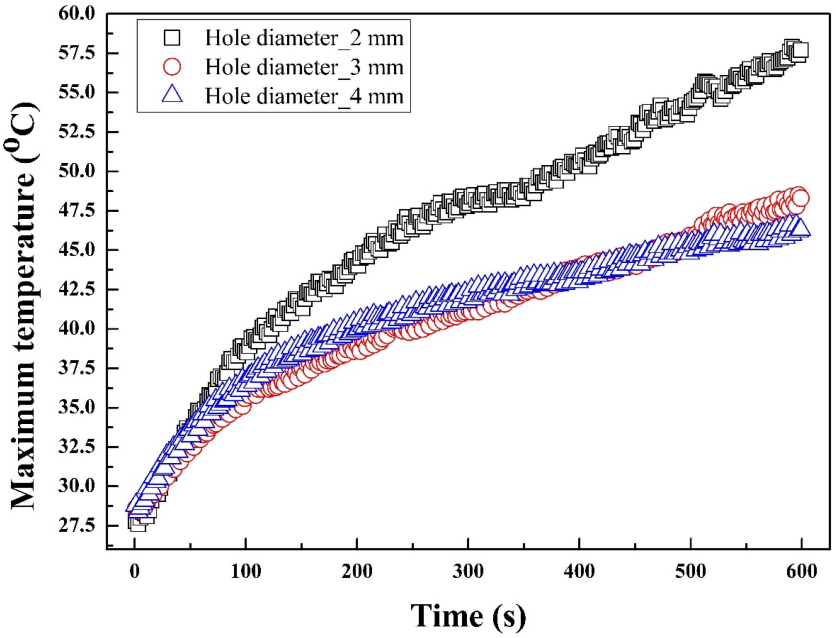

(**c**) Overload operating power of 14.21 kW

Figure 2. Maximum temperature for various dripping hole diameters under overload operating powers of (**a**) 8.28 kW, (**b**) 12.05 kW and (**c**) 14.21 kW.

3.1.3. Power Consumption

The power consumption presents the amount of injection force required to circulate the dripping oil through cooling tubes over the electric motor. The power consumption is the same for all overload operating powers; hence, the variation in the power consumption is presented for different dripping hole diameters in Figure 4. The smaller dripping hole diameter requires a higher injection pressure to spray the oil. Therefore, the power consumption increases with a decrease in the dripping hole diameter. The maximum and minimum power consumptions of 27.78 W and 18.07 W are evaluated to correspond to dripping hole diameters of 2 mm and 4 mm, respectively. The dripping hole diameter of 4 mm is suggested to develop cooling tubes for the oil-dripping cooling system based on a lower maximum temperature, higher heat transfer coefficient and lower power consumption.

3.2. Effect of Oil Flow Rate at Various Overload Operating Powers

Various heat transfer characteristics were investigated for the oil-dripping cooling system with dripping hole diameter of 4 mm by varying the oil flow rates from 8 LPM to 16 LPM under the influence of three overload operating powers.

3.2.1. Maximum Temperature

The effect of oil flow rate on maximum temperature considering three different overload operating powers is presented in Figure 5. The heat absorption rate from the electric motor to the oil increases with an increase in the oil flow rate because of the increment in the oil turbulence over the electric motor surface with a rise in oil flow rate. However, the flow distribution of the oil on the electric motor surface is also an important aspect to reduce the temperature. Therefore, the combination of a higher oil flow rate and symmetrical oil flow distribution results in an improved heat transfer rate. The oil flow rate of 12 LPM shows a better oil flow distribution that covers the maximum portion of the electric motor compared to other oil flow rates. Hence, the lowest maximum temperature is observed for the oil flow rate of 12 LPM under all overload operating powers. However, under the higher overload operating powers, the maximum temperature values are in the same range for oil flow rates of 12 LPM and 16 LPM. The lower oil flow rate of 8 LPM shows a decreased heat transfer rate and non-uniform oil flow distribution, which results in a

higher maximum temperature. To further achieve the best oil flow rate, the heat transfer coefficient is evaluated. The maximum temperatures of 36 °C, 31.9 °C and 32.5 °C in the case of an 8.28 kW overload operating power; 49.6 °C, 40.2 °C and 39.3 °C in the case of a 12.05 kW overload operating power; and 59.7 °C, 46.3 °C and 46.4 °C in the case of an 14.21 kW overload operating power are observed for oil flow rates of 8 LPM, 12 LPM and 16 LPM, respectively.

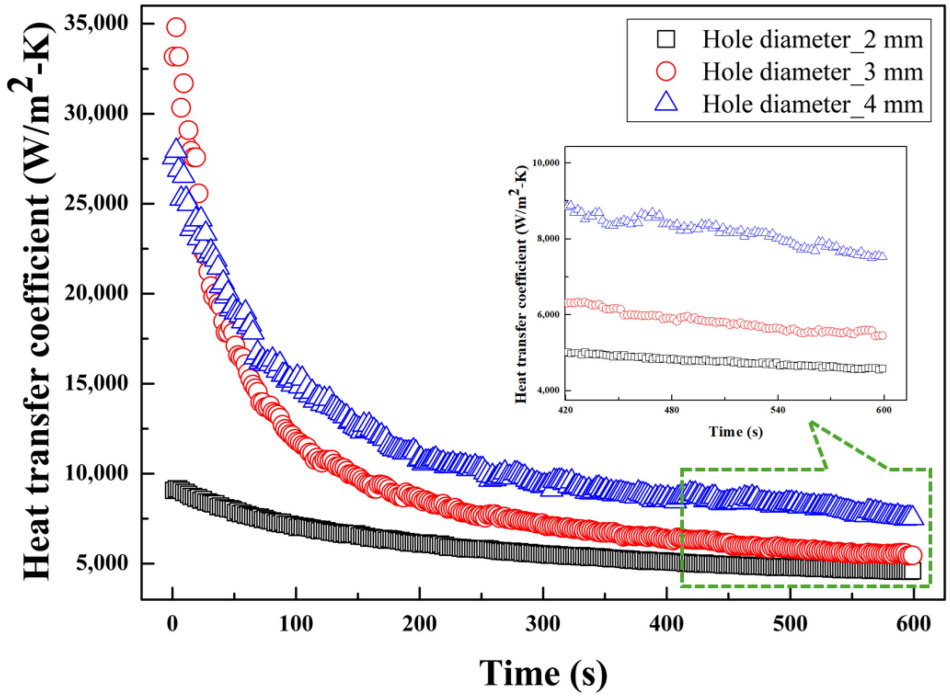

(**a**) Overload operating power of 8.28 kW

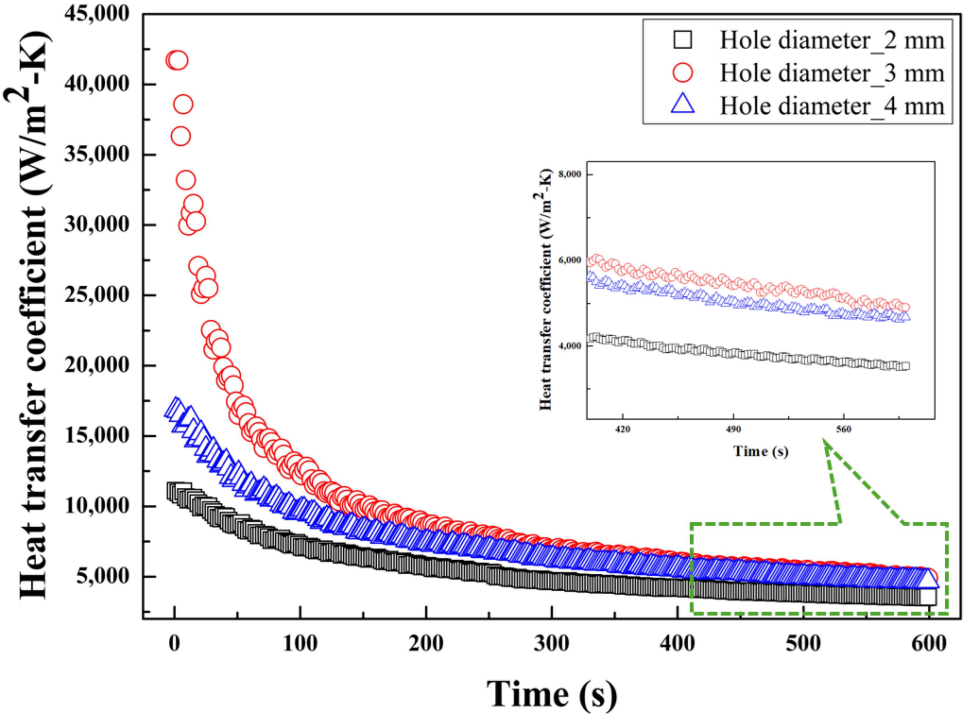

(**b**) Overload operating power of 12.05 kW

Figure 3. *Cont.*

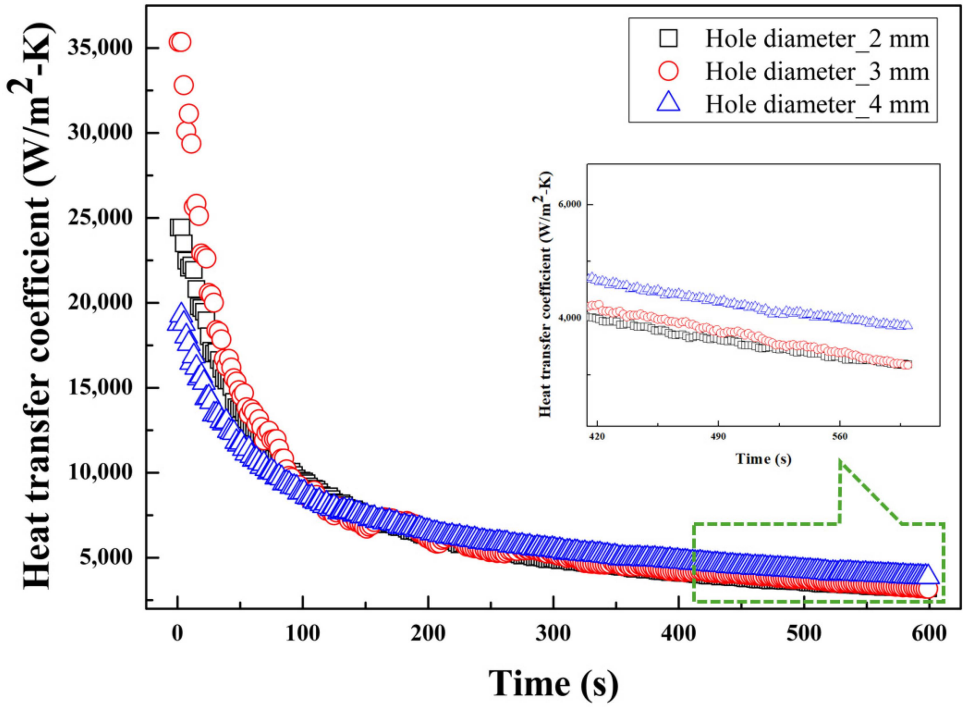

(**c**) Overload operating power of 14.21 kW

Figure 3. Heat transfer coefficient for various dripping hole diameters under overload operating powers of (**a**) 8.28 kW, (**b**) 12.05 kW and (**c**) 14.21 kW.

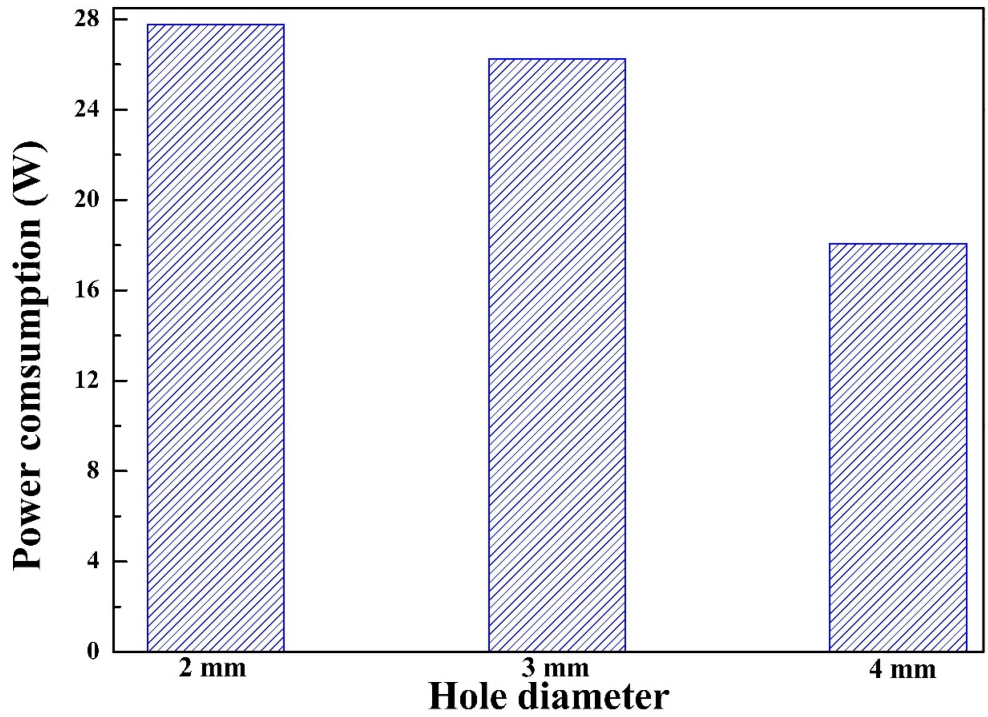

Figure 4. Power consumption for various dripping hole diameters.

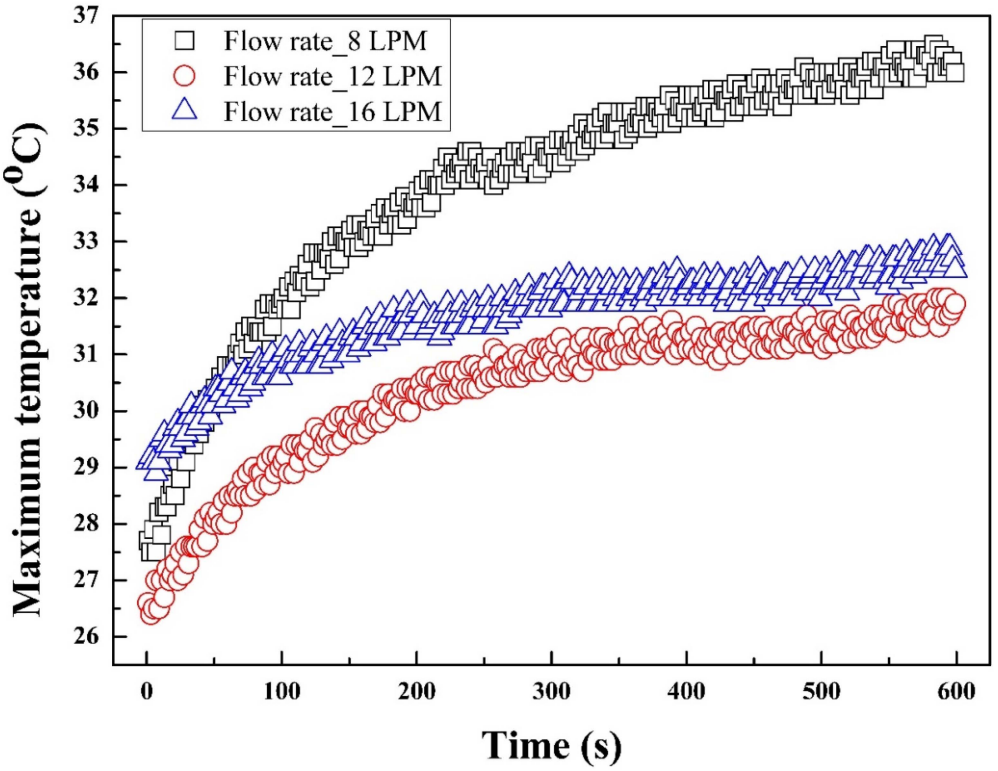

(**a**) Overload operating power of 8.28 kW

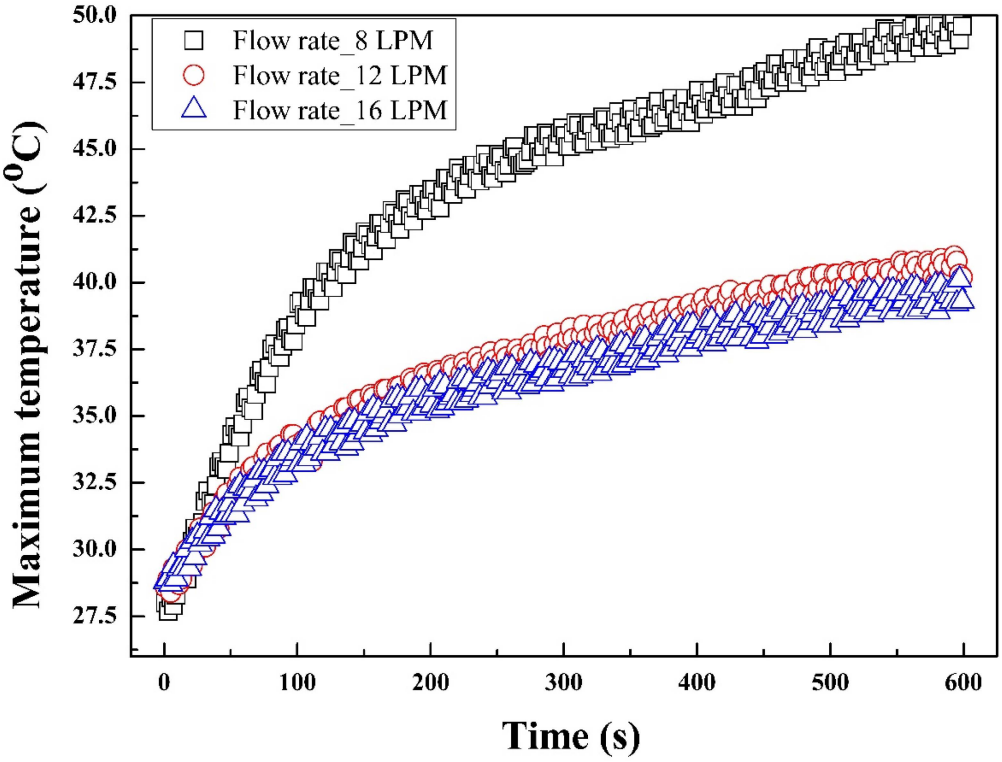

(**b**) Overload operating power of 12.05 kW

Figure 5. *Cont.*

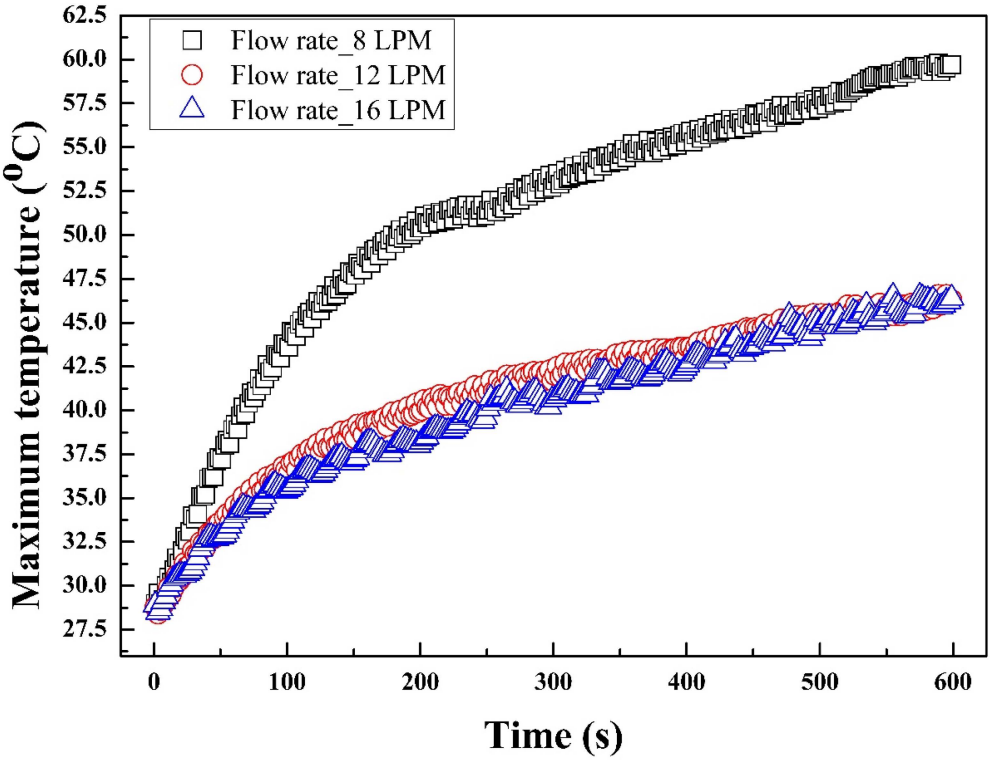

(**c**) Overload operating power of 14.21 kW

Figure 5. Maximum temperature for various oil flow rates under overload operating powers of (**a**) 8.28 kW, (**b**) 12.05 kW and (**c**) 14.21 kW.

3.2.2. Heat Transfer Coefficient

The effect of oil flow rate on heat transfer coefficient considering three overload operating powers is depicted in Figure 6. As mentioned, at higher oil flow rates, the oil turbulence, when it impacts the surface of the electric motor, is superior compared to lower oil flow rates. Therefore, the convective heat transfer from the electric motor to the oil increases with an increase in the oil flow rate. However, it should be noted that it is not necessary that a higher oil flow rate should enable a uniform oil flow distribution. Hence, the higher value of the heat transfer coefficient is evaluated for the 12 LPM oil flow rate because of the improved convective heat transfer rate and the superior oil flow distribution compared to other oil flow rates considering all overload operating powers. At higher overload operating powers, the difference in heat transfer coefficient values between oil flow rates of 12 LPM and 16 LPM is not significant. Therefore, based on the maximum temperature and heat transfer coefficients, the oil flow rate of 12 LPM is recommended. Furthermore, the amount of heat that remains unabsorbed is high at higher overload operating powers because the heat generation increases with an increase in the overload operating power. Hence, for each respective case of oil flow rate, the heat transfer coefficient decreases with an increase in the overload operating power. The heat transfer coefficients of 6118.35 W/m^2-K, 7528.61 W/m^2-K and 5897.41 W/m^2-K in the case of the 8.28 kW overload operating power; 3922.76 W/m^2-K, 4684.69 W/m^2-K and 4600.91 W/m^2-K in the case of the 12.05 kW overload operating power; and 3278.42 W/m^2-K, 3866.59 W/m^2-K and 3891.38 W/m^2-K in the case of the 14.21 kW overload operating power are evaluated for oil flow rates of 8 LPM, 12 LPM and 16 LPM, respectively.

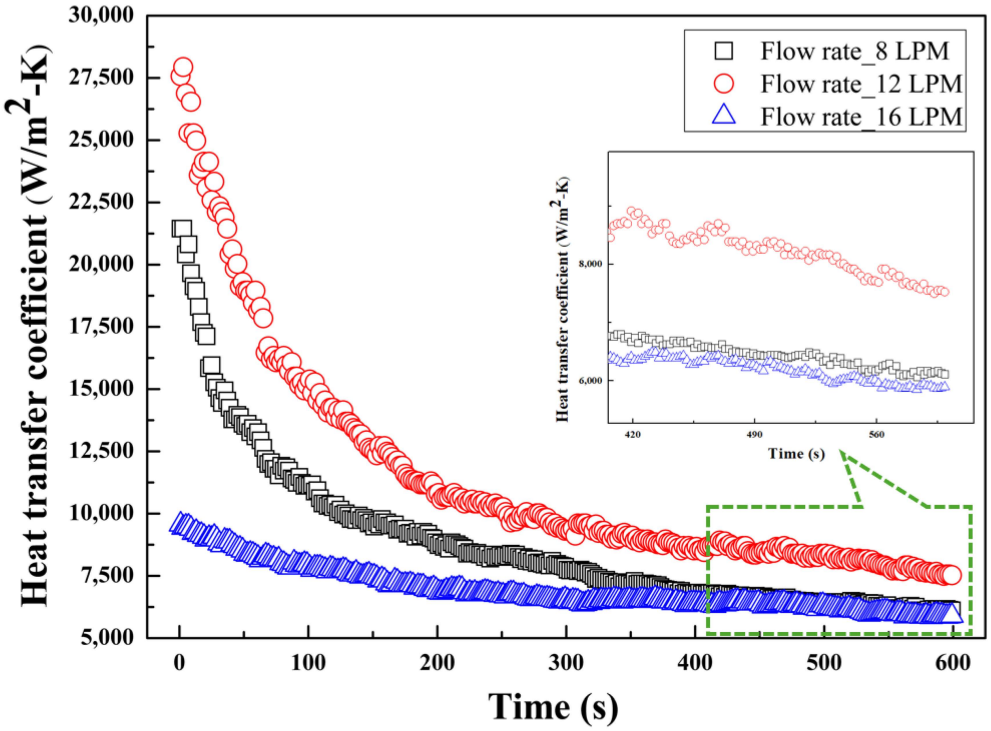

(**a**) Overload operating power of 8.28 kW

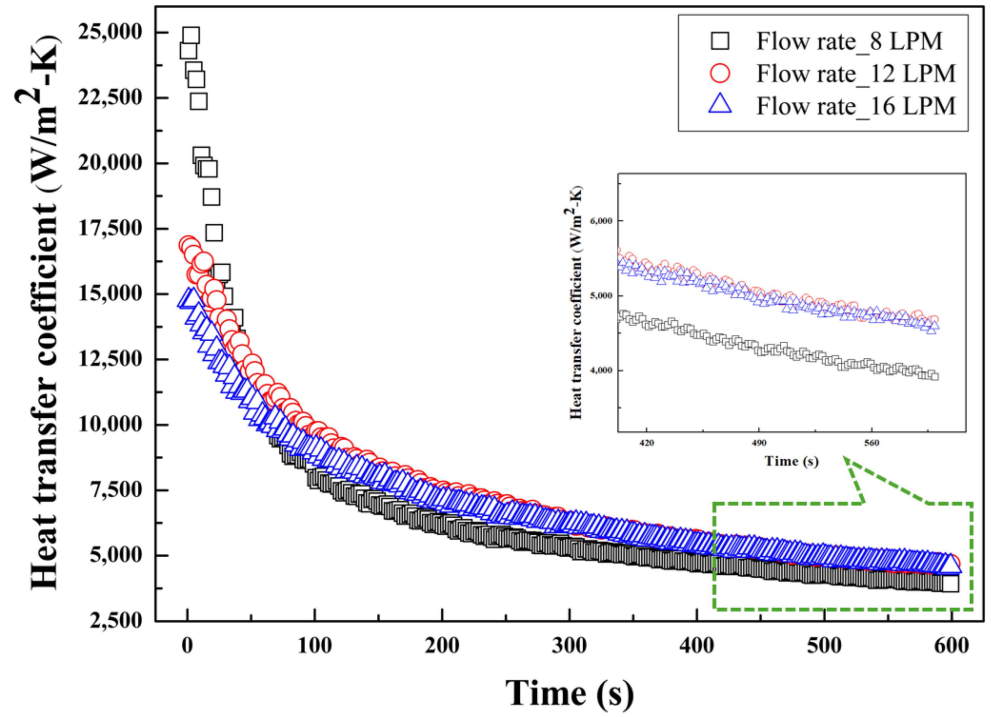

(**b**) Overload operating power of 12.05 kW

Figure 6. *Cont.*

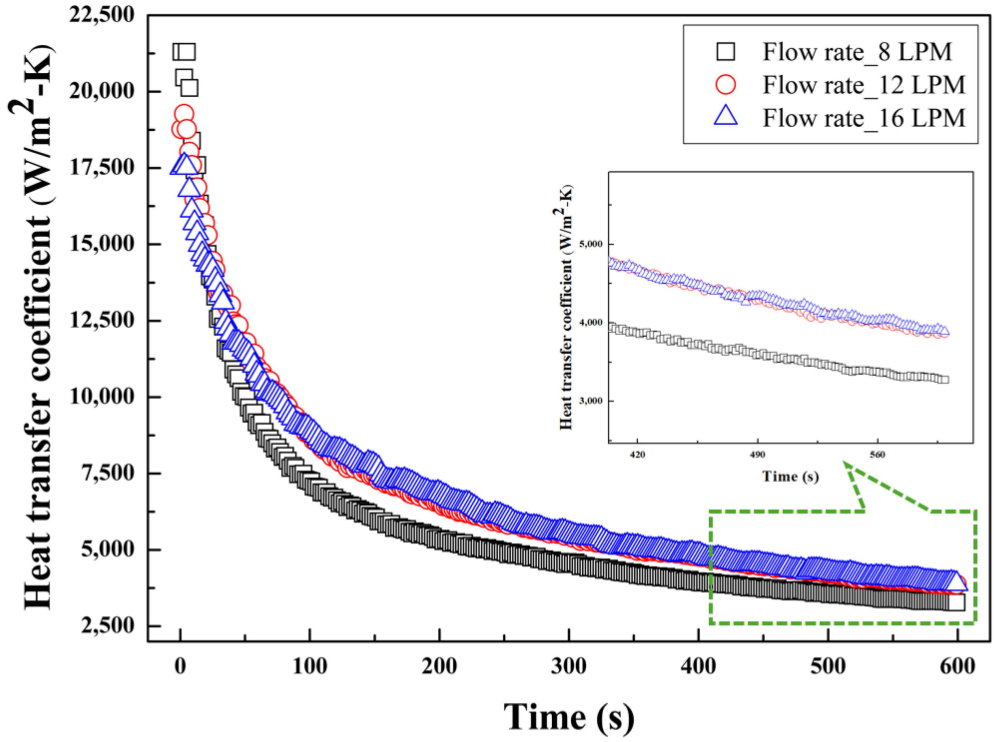

(**c**) Overload operating power of 14.21 kW

Figure 6. Heat transfer coefficient for various oil flow rates under overload operating powers of (**a**) 8.28 kW, (**b**) 12.05 kW and (**c**) 14.21 kW.

3.2.3. Power Consumption

The effect of a change in oil flow rate on power consumption is shown in Figure 7. The injection pressure indicates the impact force at which the oil drips from the cooling tube onto the electric motor surface. When the flow rate of the oil increases, the oil circulates at a faster rate through the cooling tubes, which means the impact force created by the dripping oil on the surface of the electric motor is enhanced and, thus, results in a high injection pressure at higher oil flow rates. Also, the faster circulation of the oil at the higher flow rate makes the pump motor consume more energy. Hence, the power consumption increases with an increase in the oil flow rate because compensating for the higher drag force owing to the superior oil mixing at higher oil flow rates demands an increment in injection pressure. The oil flow rates of 8 LPM and 16 LPM show minimum and maximum power consumptions of 17.32 W and 37.75 W, respectively. The power consumption in the case of the 12 LPM oil flow rate is observed as 18.06 W, which is not significantly higher compared to the minimum power consumption. The heat transfer coefficient, as an indication of cooling effectiveness, is superior at the oil flow rate of 12 LPM compared to other oil flow rates. Furthermore, the power consumption at the 12 LPM oil flow rate is much lower than that at the 16 LPM oil flow rate, and the value is in the same range as that of the lowest power consumption observed at the 8 LPM oil flow rate. Therefore, considering the trade-off between improved heat transfer coefficient and a lower power consumption, the oil flow rate of 12 LPM is suggested to be adopted for an oil-dripping cooling system.

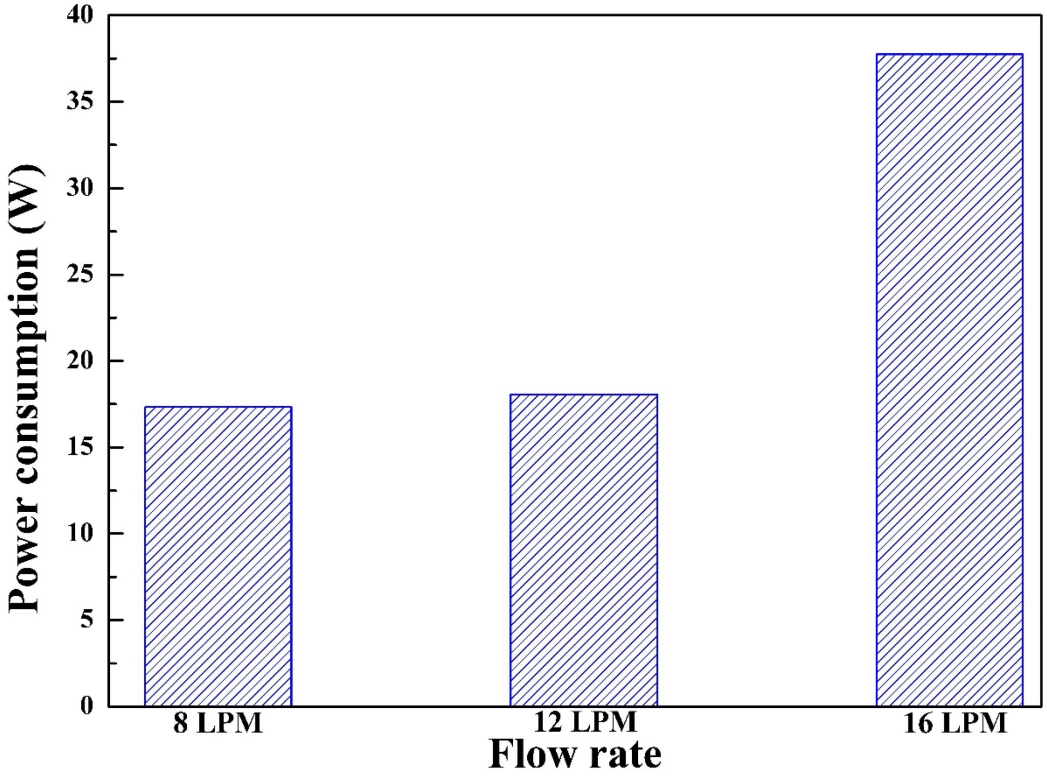

Figure 7. Power consumption for various oil flow rates.

4. Conclusions

An electric motor with an oil-dripping cooling was experimentally investigated for various heat transfer characteristics of maximum temperature, heat transfer coefficient and power consumption considering various conditions of dripping hole diameter, oil flow rate and overload operating power. The following key findings have been added to the reference database for the spray cooling of electric motors:

(a) The maximum temperature decreased with an increase in the dripping hole diameter such that the lowest maximum temperature was observed for a dripping hole diameter of 4 mm under all overload operating powers. The lowest maximum temperatures of 31.9 °C, 40.2 °C and 46.3 °C were observed for a dripping hole diameter of 4 mm in the case of overload operating powers of 8.28 kW, 12.05 kW and 14.21 kW, respectively.

(b) Higher values of heat transfer coefficient were found for a dripping hole diameter of 4 mm, and with the increase in the overload operating power, the heat transfer coefficient showed a decrement in its values. The heat transfer coefficients of 7528.61 W/m^2-K, 4684.69 W/m^2-K and 3866.59 W/m^2-K were evaluated for the 4 mm dripping hole diameter at overload operating powers of 8.28 kW, 12.05 kW and 14.21 kW, respectively. The power consumption decreased with an increase in the dripping hole diameter.

(c) The oil flow rates of 12 LPM and 16 LPM depicted a lower maximum temperature and higher heat transfer coefficient. However, the power consumptions reported at corresponding oil flow rates were 18.06 W and 37.75 W.

(d) The combination of a 4 mm dripping hole diameter and a 12 LPM oil flow rate is recommended for oil-dripping cooling systems to achieve enhanced heat transfer characteristics of an electric motor.

The effect of design parameters on heat dissipation performance is summarized in the present study which could be added to the reference database while developing the oil-dripping cooling system for electric motors. The proposed concept could be generalized to design a direct oil cooling system for high-power density components such as data

centers and power electronics; however, structural adjustments should be made based on the configuration of the target devices. In order to commercialize the oil-dripping cooling system for electric-vehicle motors, further research studies should be added to the open literature to ensure its reliability under actual and robust operating conditions. In future work, housing with oil-dripping cooling will be developed to test the thermal management performance and safety of electric-vehicle motors under real driving conditions.

Author Contributions: Conceptualization, E.-H.K., K.S.G. and M.-Y.L.; methodology, E.-H.K. and K.S.G.; formal analysis, E.-H.K.; investigation, E.-H.K.; resources, E.-H.K., K.S.G., S.C.P. and M.-Y.L.; data curation, E.-H.K.; writing—original draft preparation, E.-H.K. and K.S.G.; writing—review and editing, E.-H.K., K.S.G., S.C.P. and M.-Y.L.; visualization, E.-H.K. and K.S.G.; supervision, M.-Y.L.; project administration, M.-Y.L.; funding acquisition, M.-Y.L. All authors have read and agreed to the published version of the manuscript.

Funding: This work was supported by the Dong-A University research fund.

Data Availability Statement: The data presented in this study will be available on request to the corresponding author.

Conflicts of Interest: The authors declare no conflicts of interest.

References

1. Alanazi, F. Electric Vehicles: Benefits, Challenges, and Potential Solutions for Widespread Adaptation. *Appl. Sci.* **2023**, *13*, 6016. [CrossRef]
2. Ramraj, R.; Pashajavid, E.; Alahakoon, S.; Jayasinghe, S. Quality of Service and Associated Communication Infrastructure for Electric Vehicles. *Energies* **2023**, *16*, 7170. [CrossRef]
3. Popescu, M.; Riviere, N.; Volpe, G.; Villani, M.; Fabri, G.; di Leonardo, L. A Copper Rotor Induction Motor Solution for Electrical Vehicles Traction System. In Proceedings of the IEEE Energy Conversion Congress and Exposition (ECCE 2019), Baltimore, MD, USA, 29 September–3 October 2019; pp. 3924–3930.
4. Lucas, S.; Bari, S.; Marian, R.; Lucas, M.; Chahl, J. Cooling by Peltier effect and active control systems to thermally manage operating temperatures of electrical Machines (Motors and Generators). *Therm. Sci. Eng. Prog.* **2022**, *27*, 100990. [CrossRef]
5. Tola, O.J.; Ambafi, J.G.; Umoh, E.A.; Osinowo, O.E. Performance analysis of a pmsm for traction applications in electric vehicles with hairpin winding technology. In Proceedings of the IEEE Nigeria 4th International Conference on Disruptive Technologies for Sustainable Development (NIGERCON 2022), Lagos, Nigeria, 5–7 April 2022; pp. 1–5.
6. Ha, T.; Kim, D.K. Study of injection method for maximizing oil-cooling performance of electric vehicle motor with hairpin winding. *Energies* **2021**, *14*, 747. [CrossRef]
7. Wang, X.; Li, B.; Gerada, D.; Huang, K.; Stone, I.; Worrall, S.; Yan, Y. A critical review on thermal management technologies for motors in electric cars. *Appl. Therm. Eng.* **2022**, *201*, 117758. [CrossRef]
8. Momen, F.; Rahman, K.; Son, Y. Electrical propulsion system design of Chevrolet Bolt battery electric vehicle. *IEEE Trans. Ind. Appl.* **2018**, *55*, 376–384. [CrossRef]
9. Yang, Y.; Bilgin, B.; Kasprzak, M.; Nalakath, S.; Sadek, H.; Preindl, M.; Emadi, A. Thermal management of electric machines. *IET Electr. Syst. Transp.* **2017**, *7*, 104–116. [CrossRef]
10. Yang, X.; Fatemi, A.; Nehl, T.; Hao, L.; Zeng, W.; Parrish, S. Comparative study of three stator cooling jackets for electric machine of mild hybrid vehicle. *IEEE Trans. Ind. Appl.* **2020**, *57*, 1193–1201. [CrossRef]
11. Liu, M.; Li, Y.; Ding, H.; Sarlioglu, B. Thermal management and cooling of windings in electrical machines for electric vehicle and traction application. In Proceedings of the IEEE Transportation Electrification Conference and Expo (ITEC 2017), Chicago, IL, USA, 22–24 June 2017; pp. 668–673.
12. Acquaviva, A.; Skoog, S.; Thiringer, T. Design and verification of in-slot oil-cooled tooth coil winding PM machine for traction application. *IEEE Trans. Ind. Electron.* **2020**, *68*, 3719–3727. [CrossRef]
13. Lindh, P.; Petrov, I.; Jaatinen-Värri, A.; Grönman, A.; Martinez-Iturralde, M.; Satrústegui, M.; Pyrhönen, J. Direct liquid cooling method verified with an axial-flux permanent-magnet traction machine prototype. *IEEE Trans. Ind. Electron.* **2017**, *64*, 6086–6095. [CrossRef]
14. Venturini, G.; Volpe, G.; Villani, M.; Popescu, M. Investigation of cooling solutions for hairpin winding in traction application. In Proceedings of the International Conference on Electrical Machines (ICEM 2020), Gothenburg, Sweden, 23–26 August 2020; Volume 1, pp. 1573–1578.
15. Venturini, G.; Volpe, G.; Popescu, M. Slot water jacket cooling system for traction electrical machines with hairpin windings: Analysis and comparison. In Proceedings of the IEEE International Electric Machines & Drives Conference (IEMDC 2021), Hartford, CT, USA, 17–20 May 2021; pp. 1–6.
16. Park, J.; An, J.; Han, K.; Choi, H.S.; Park, I.S. Enhancement of cooling performance in traction motor of electric vehicle using direct slot cooling method. *Appl. Therm. Eng.* **2022**, *217*, 119082. [CrossRef]

17. Huang, Z.; Nategh, S.; Lassila, V.; Alaküla, M.; Yuan, J. Direct oil cooling of traction motors in hybrid drives. In Proceedings of the IEEE International Electric Vehicle Conference (IEVC 2012), Greenville, SC, USA, 4–8 March 2012; pp. 1–8.
18. Zhang, F.; Gerada, D.; Xu, Z.; Liu, C.; Zhang, H.; Zou, T.; Gerada, C. A thermal modeling approach and experimental validation for an oil spray-cooled hairpin winding machine. *IEEE Trans. Transp. Electrif.* **2021**, *7*, 2914–2926. [CrossRef]
19. Tikadar, A.; Joshi, Y.; Kumar, S. Comparison between Direct Winding Heat Exchanger and Slot-liner Confined Evaporative Cooling of Electric Motor. In Proceedings of the 21st IEEE Intersociety Conference on Thermal and Thermomechanical Phenomena in Electronic Systems (iTherm 2022), San Diego, CA, USA, 31 May–3 June 2022; pp. 1–10.
20. Davin, T.; Pellé, J.; Harmand, S.; Yu, R. Experimental study of oil cooling systems for electric motors. *Appl. Therm. Eng.* **2015**, *75*, 1–13. [CrossRef]
21. Ponomarev, P.; Polikarpova, M.; Pyrhönen, J. Thermal modeling of directly-oil-cooled permanent magnet synchronous machine. In Proceedings of the International Conference on Electrical Machines (ICEM 2012), Marseille, France, 2–5 September 2012; pp. 1882–1887.
22. La Rocca, A.; Zou, T.; Moslemin, M.; Gerada, D.; Gerada, C.; Cairns, A. Thermal modelling of a liquid cooled traction machine with 8-layer hairpin windings. In Proceedings of the IECON 2021–47th Annual Conference of the IEEE Industrial Electronics Society, Toronto, ON, Canada, 13–16 October 2021; pp. 1–6.
23. Guechi, M.R.; Desevaux, P.; Baucour, P.; Espanet, C.; Brunel, R.; Poirot, M. On the improvement of the thermal behavior of electric motors. In Proceedings of the IEEE Energy Conversion Congress and Exposition (ECCE 2013), Denver, CO, USA, 15–19 September 2013; pp. 1512–1517.
24. Wang, J.X.; Li, Y.Z.; Yu, X.K.; Li, G.C.; Ji, X.Y. Investigation of heat transfer mechanism of low environmental pressure large-space spray cooling for near-space flight systems. *Int. J. Heat Mass Transf.* **2018**, *119*, 496–507. [CrossRef]
25. Available online: https://www.hyundai-lube-me.com/product/xteer-atf-sp4/ (accessed on 17 August 2023).
26. Liu, L.; Wang, X.; Ge, M.; Zhao, Y. Experimental study on heat transfer and power consumption of low-pressure spray cooling. *Appl. Therm. Eng.* **2021**, *184*, 116253. [CrossRef]
27. Chong, Y.C.; Goss, J.; Popescu, M.; Staton, D.; Liu, C.; Gerada, D.; Gerada, C. Experimental characterisation of radial oil spray cooling on a stator with hairpin windings. In Proceedings of the 10th International Conference on Power Electronics, Machines and Drives (PEMD 2020), Online, 15–17 December 2020; Volume 2020, pp. 879–884.
28. Available online: https://www.energy.gov/sites/prod/files/2014/04/f15/10097517.pdf (accessed on 13 November 2023).
29. Heat Transfer in Electric Machines. Available online: www.eomys.com (accessed on 9 November 2023).
30. Garud, K.S.; Hwang, S.G.; Han, J.W.; Lee, M.Y. Performance characteristics of the direct spray oil cooling system for a driving motor of an electric vehicle. *Int. J. Heat Mass Transf.* **2022**, *196*, 123228. [CrossRef]
31. Garud, K.S.; Seo, J.H.; Bang, Y.M.; Pyo, Y.D.; Cho, C.P.; Lee, M.Y.; Lee, D.Y. Energy, exergy, environmental sustainability and economic analyses for automotive thermoelectric generator system with various configurations. *Energy* **2022**, *244*, 122587. [CrossRef]
32. Seo, J.H.; Garud, K.S.; Lee, M.Y. Grey relational based Taguchi analysis on thermal and electrical performances of thermoelectric generator system with inclined fins hot heat exchanger. *Appl. Therm. Eng.* **2021**, *184*, 116279. [CrossRef]
33. Raj, A.K.; Srinivas, M.; Jayaraj, S. A cost-effective method to improve the performance of solar air heaters using discrete macro-encapsulated PCM capsules for drying applications. *Appl. Therm. Eng.* **2019**, *146*, 910–920. [CrossRef]